Hydrol. Earth Syst. Sci. Discuss., 12, 2081–2112, 2015
www.hydrol-earth-syst-sci-discuss.net/12/2081/2015/
doi:10.5194/hessd-12-2081-2015

Hydrology and Earth System Sciences
Discussions

Comparing TRMM 3B42, CFSR and ground-based rainfall estimates as input for hydrological models, in data scarce regions: the Upper Blue Nile Basin, Ethiopia

A. W. Worqlul[1,2,3], A. S. Collick[4], S. A. Tilahun[3], S. Langan[2], T. H. M. Rientjes[5], and T. S. Steenhuis[1,3]

[1]Department of Biological and Environmental Engineering, Cornell University, Ithaca, New York, USA
[2]International Water Management Institute, Addis Ababa, Ethiopia
[3]School of Civil and Water Resource Engineering, Bahir Dar University, Bahir Dar, Ethiopia
[4]USDA-ARS, University Park, Pennsylvania, USA
[5]Department of Water Resources, Faculty of Geo-information Science and Earth Observation (ITC), University of Twente, Enschede, the Netherlands

Received: 27 December 2014 – Accepted: 1 February 2015 – Published: 18 February 2015

Correspondence to: T. S. Steenhuis (tss1@cornell.edu)

Published by Copernicus Publications on behalf of the European Geosciences Union.

Abstract

Accurate prediction of hydrological models requires accurate spatial and temporal distribution of rainfall observation network. In developing countries rainfall observation station network are sparse and unevenly distributed. Satellite-based products have the potential to overcome these shortcomings. The objective of this study is to compare the advantages and the limitation of commonly used high-resolution satellite rainfall products as input to hydrological models as compared to sparsely populated network of rain gauges. For this comparison we use two semi-distributed hydrological models Hydrologiska Byråns Vattenbalansavdelning (HBV) and Parameter Efficient Distributed (PED) that performed well in Ethiopian highlands in two watersheds: the Gilgel Abay with relatively dense network and Main Beles with relatively scarce rain gauge stations. Both are located in the Upper Blue Nile Basin. The two models are calibrated with the observed discharge from 1994 to 2003 and validated from 2004 to 2006. Satellite rainfall estimates used includes Climate Forecast System Reanalysis (CFSR), Tropical Rainfall Measuring Mission (TRMM) 3B42 version 7 and ground rainfall measurements. The results indicated that both the gauged and the CFSR precipitation estimates were able to reproduce the stream flow well for both models and both watershed. TRMM 3B42 performed poorly with Nash Sutcliffe values less than 0.1. As expected the HBV model performed slightly better than the PED model, because HBV divides the watershed into sub-basins resulting in a greater number of calibration parameters. The simulated discharge for the Gilgel Abay was better than for the less well endowed (rain gauge wise) Main Beles. Finally surprisingly, the ground based gauge performed better for both watersheds (with the exception of extreme events) than TRMM and CFSR satellite rainfall estimates. Undoubtedly in the future, when improved satellite products will become available, this will change.

1 Introduction

Sound predictions of hydrological models need accurate spatial and temporal distribution of precipitation (Sharma et al., 2012). However, in developing countries ground rainfall observation stations are often unevenly and sparsely distributed and unlikely to improve soon (Worqlul et al., 2014). According to the World Meteorological Organization (WMO, 1994) the minimum rainfall station network density for tropical regions is 600 to 900 km^2 per station for flat areas and 100 to 250 km^2 per station for mountainous regions. But, in developing countries such a dense network is not available (Taye and Willems, 2012; Conway, 2000). Recently, the availability of satellite rainfall estimation where there is limited or no conventional ground rainfall observation stations has attracted the interest of hydrologists (Collischonn et al., 2008; Yilmaz et al., 2005; Hong et al., 2007). Satellite rainfall estimates have the advantage of high temporal resolution and spatial coverage, even over mountainous regions and sparsely populated areas.

Rainfall products, the Climate Forecast System Reanalysis (CFSR) and Tropical Rainfall Measuring Mission (TRMM) 3B42 version 7 (hereafter, simply "TRMM"), besides being widely used and freely available in Africa, have a relatively high spatial resolution, global coverage and high temporal resolution. The product TRMM 3B42 has been available since 1998 in a spatial resolution of $0.25^\circ \times 0.25^\circ$ grid (≈ 27 km at the equator) at a 3 hourly temporal resolution in a global belt extending from 50° N to 50° S. The CFSR global atmosphere data has a spatial resolution of approximately 38 km and the data is available since 1979 (Saha et al., 2010). Detail information on TRMM and CFSR data can be found in (Worqlul et al., 2014; Wang et al., 2011; Saha et al., 2010). The validation of satellite rainfall products can be achieved by direct comparison with the ground observation station network (Dinku et al., 2008; Bitew et al., 2012; Worqlul et al., 2014) or by their ability to predict stream flow using hydrological models (Bitew et al., 2012; Fuka et al., 2014). A variety of hydrology models applied in the Ethiopian highlands, such as the Agricultural Non-Point Source Pollution (AGNPS) (Haregeweyn and Yohannes, 2003; Mohammed et al., 2004), Water Erosion Prediction Project (WEPP) (Zeleke, 2000) and the Soil and Water Assessment Tool (SWAT) (Setegn et al., 2008, 2009, 2010; Betrie et al., 2011), had limitations in capturing the daily runoff dynamics because the underlying runoff mechanism in these models is based on infiltration excess although experimentally it has been shown that saturation excess is the dominant mechanism of generating overland flow (Bayabil et al., 2010; Tilahun et al., 2013a, b). Water balance models, in particular the Parameter Efficient Distributed (PED) (Steenhuis et al., 2009) and the Hydrologiska Byråns Vattenbalansavdelning (HBV) (Lindström et al., 1997), which include saturation excess processing and are not input data intensive, could represent the runoff better in monsoon climates than infiltration excess runoff models for scales ranging from 100 ha basin to the whole Blue Nile basin (Tilahun et al., 2013a, b, c; 2014; Steenhuis et al., 2015; Abdo et al., 2009; Wale et al., 2009).

Therefore, using the PED and HBV models to simulate stream flow, we assessed the suitability (performance) and the limitations of state-of-the-art high-resolution satellite rainfall products readily available in Africa in two watersheds, Gilgel Abay and Main Beles, located in the upper Blue Nile Basin, Ethiopia. Gilgel Abay basin has high quality discharge data and a relatively well distributed network of ground rainfall observation station, and Main Beles basin also has good quality discharge data, but a less well endowed network of ground rainfall stations with a long period daily record data.

2 Methodology

2.1 Study area description

The study watersheds, Gilgel Abay and Main Beles, are located in the Blue Nile Basin, in the western part of the Ethiopian highland. The Gilgel Abay watershed is located in the Tana basin, between 10°56′ and 11°58′ N latitude and 36°44′ and 37°34′ E longitudes. Gilgel Abay River is the source of Lake Tana; it originates from a small spring located near Gish Abay Mountain at elevation of 3000 m a.m.s.l. The Main Beles wa-

tershed is located in the Beles basin, geographically it extends from 10°56′ to 12° N latitude and 35°12′ to 37° E longitude. The watershed areas of the Gilgel Abay and Main Beles at their gauging sites are approximately 1650 km^2 and 3212 km^2, respectively, extracted from the 90 m resolution Shuttle Radar Topographic Mission (SRTM) Digital Elevation Model (DEM). In Fig. 1, the location of meteorological stations and drainage pattern of the Gilgel Abay and Main Beles sub-basins are depicted.

Gilgel Abay and Main Beles basins have a complex topography with a significant elevation variation ranging from 1890 to 3530 and 990 to 2725 m, respectively. The slope of the watersheds varies from zero to 140 %, with an average slope of 12 % for Gilgel Abay and 14 % for Main Beles basins. Approximately 50 % of the watersheds have a slope less than 8 %. Gilgel Abay and Main Beles basins have an average annual rainfall of 1860 and 1550 mm, respectively. The main rainfall season is from June to September and accounts for 70 to 90 % of the annual rainfall (Kebede et al., 2006; Tarekegn and Tadege, 2006).

2.2 Climatological and discharge data

Daily precipitation is collected from Ethiopian Meteorological Agency (EMA) for multiple stations. Daily data from 1994 to 2006 is obtained from Dangila, Adet, Sekela and Enjibara stations and the data collected from Chagni and Pawi was from 1998 to 2006. In addition, the only data needed to estimate potential evaporation such as maximum and minimum temperature, daily sunshine hour, maximum and minimum humidity and wind speed was available at the Dangila station. Daily discharge data for Gilgel Abay and Main Beles at the outlet stations from 1994 to 2006 was obtained from Ethiopian Ministry of Water, Irrigation and Energy. The daily gridded satellite rainfall estimation data TRMM product (3B42) Version 7 was downloaded from the ftp server at http://gdata1.sci.gsfc.nasa.gov/daac-bin/G3/gui.cgi?instance_id=TRMM_3B42_Daily and CFSR at http://rda.ucar.edu/datasets/ds094.1/.

2.3 Methods

The study is comprised of two parts, in the first part, after estimating the areal long-term monthly rainfall estimates of gauged rainfall, CFSR and TRMM data from 1994–2006 for Gilgel Abay and Main Beles basins a comparison is done by using simple standard statistics (i.e., coefficient of determination). The gauged rainfall data is interpolated by Thiessen Polygon method. Next, the high-resolution satellite rainfall products (CFSR and TRMM) and gauged rainfall daily data are used as an input to two watershed models HBV-IHMS and PED for daily stream flow simulation in the Gilgel Abay and Main Beles basins. The model parameters are used to fit the observed flow through model calibration. The model calibration period ranges from 1994 to 2003 and the model is validated from 2004 to 2006 for gauged rainfall, CFSR and TRMM data. The performance of the calibrated model is evaluated by the Nash–Sutcliffe Coefficient (NSE), percent bias (PBIAS), and coefficient of determination (R^2). The hydrological models HBV and PED are described below:

HBV-IHMS model

The HBV (Hydrologiska Byråns Vattenbalansavdelning) model (Lindström et al., 1997) is a conceptual rainfall–runoff model for continuous daily simulation of catchment runoff. In HBV, the watershed is divided into sub-watersheds and further divided into elevation and land use zones. The model simulates daily runoff using daily rainfall, temperature, long-term average monthly potential evaporation, geographical information of the catchment which is sliced elevation crossed with land use and observed runoff data for calibration. The general water balance is described in Eq. (1):

$$P - E - Q = \frac{\mathrm{d}}{\mathrm{d}t}[\mathrm{SP} + \mathrm{SM} + \mathrm{UZ} + \mathrm{LZ} + L], \tag{1}$$

where P is the precipitation, E is evapotranspiration, Q is runoff, SP is snow pack, SM is soil moisture, UZ is upper ground zone, LZ is lower ground zone, and L is the lake volume.

The model consists of subroutines for precipitation, soil moisture accounting, response routine, transformation function and simple routing procedure. The soil moisture accounting routine is based on three parameters, Beta (β), FC and LP. β controls the contribution to the response function from each millimetres of rainfall. FC is the maximum soil moisture storage. As the soil moisture exceeds the limit for potential evaporation (LP), water will evaporate at a potential rate. The response routine is described by upper non-linear reservoir and a linear lower response routine connected with the upper box with Percolation (PERC). K and K4 are recession coefficient parameters for the upper and lower response parameters. The non-linearity of the upper reservoir is controlled by the parameter Alpha (α). The higher α the higher the peaks and the quicker the recession (SHMI, 2006). A complete description of the HBV model can be found in Lindström et al. (1997), SMHI (2006) and Wale et al. (2009) among others. Input for HBV includes: long-term monthly potential evaporation is estimated by the Penman-combination equation using Dangila meteorological station. A digital elevation model (DEM) from SRTM DEM (Jarvis et al., 2008) is used to extract the drainage area of the watersheds and to divide each watershed into three different sub-basins and elevations zones. Land use data is collected from Ethiopia Ministry of Water, Irrigation and Energy.

PED model

The PED (Parameter Efficient Distributed) model (Steenhuis et al., 2009) is a conceptual semi-distributed rainfall–runoff model for continuous daily simulation of catchment runoff. In PED the watershed is subdivided into three sub-regions distinguished as the bottom lands that potentially saturate in the rainy monsoon phase, degraded hillslope/exposed rock with little or no soil cover and permeable hillslopes (infiltration zones). In the PED model various portions of the watershed become hydrologically active when threshold moisture content is exceeded (Steenhuis et al., 2013). The permeable hillslopes/infiltration zones contribute to the rapid subsurface flow (called interflow) characterised by flow decreasing as a linear function of time, and baseflow is characterised by an exponentially decreasing flow in time Steenhuis et al. (2013). Overland flow is generated from saturated areas in the relatively flatter areas in the landscape and areas where bed rock is exposed Steenhuis et al. (2009). For each of the three regions, the water balance calculation is based on Thornthwaite and Mather (1955) procedure. The general water balance equation for the sub-regions is described under Eq. (2):

$$S_t = S_{t-\Delta t} + (P - \mathrm{AET} - R - \mathrm{Perc})\Delta t, \qquad (2)$$

where S_t is water stored in the topmost layer, $S_{t-\Delta t}$ is the previous time step storage (mm), P is precipitation (mm day^{-1}), AET is the actual evapotranspiration, R is the saturation excess runoff (mm day^{-1}), Perc is the percolation to the subsoil (mm day^{-1}), and Δt is the time step (day).

The model simulates the daily runoff using daily rainfall, potential evaporation and daily runoff data for calibration. Input for PED: potential evaporation is estimated by the Penman-combination equation. Landscape parameter for the model, the relative area of three regions are used as a model calibration parameter with their respective maximum soil moisture storage capacity. Subsurface flow is simulated using a linear reservoir with a half-life ($t_{1/2}$) and interflow employing a zero order reservoir calibration parameter τ^* is the duration of the period after a single rainstorm until interflow ceases. A complete description of the PED model can be found in Steenhuis et al. (2009), Tesemma et al. (2010), and Tilahun et al. (2013b).

2.4 Model calibration and validation

The two simulation models were calibrated manually, first by fitting the runoff volumes followed by calibrating the shape of the hydrograph from 1994 to 2003 for gauged

rainfall and CFSR data. The TRMM data is calibrated from 1998 to 2003. The calibrated model is validated from 2004 to 2006 in all cases.

The model performance is evaluated by three objective functions consisting of the Nash–Sutcliffe Efficiency (NSE) (Nash and Sutcliffe, 1970), percent bias (PBIAS), and coefficient of determination (R^2). NSE is a normalized statistic that determines the relative magnitude of the residual variance compared to the measured observed flow variance. NSE ranges from negative infinite to 1. Generally, NSE value between 0.6 and 0.8 indicates fair to good performance and a model is said to be very good when NSE is above 0.8 (Moriasi et al., 2007). PBIAS is the relative difference between the observed and simulated flows. PBIAS measures the tendency of the average simulated flow to be larger or smaller than the observed flow (Gupta et al., 1999). R^2 is used to evaluate the goodness of fit of the relations. R^2 examines the degree of linear association between the observed and simulated flows.

3 Results and discussion

3.1 Comparsion of areal gauged rainfall with TRMM and CFSR rainfall estimates

The areal rainfall of the gauged rainfall is estimated by Thiessen Polygon method with relative areas for each of the six rain gauges as shown in Fig. 2. Figure 3 indicates the satellite rainfall observation grid generated from TRMM and CFSR data for Gilgel Abay and Main Beles basins. The long-term monthly areal average ground observed rainfall, TRMM and CFSR for the Gilgel Abay and Main Beles basins are depicted in Fig. 4. The CFSR satellite rainfall and gauged data are averaged over the period from 1994 to 2006 and TRMM over the period from 1998 to 2006 for the Gilgel Abay and Main Beles basins.

Gilgel Abay and Main Beles watersheds have similar rainfall patterns according to both gauged and CFSR rainfall data with a goodness of fit, R^2, of 0.98 for each (Table 1). Areal TRMM rainfall estimates for Gilgel Abay and Main Beles have a similar pattern indicated by R^2, of 0.90. CFSR also has captured the gauged rainfall for Gilgel Abay and Main Beles with R^2 values of 0.92 and 0.90, respectively. The fit between TRMM and gauged data is poor, 0.35 and 0.12 for Gilgel Abay and Main Beles, respectively. TRMM average annual rainfall volume estimates underpredict by 13 and 2 % for Gilgel Abay and Main Beles, respectively, while CFSR data overpredicts by 20 and 36 %, respectively. Seventy five percent of the gauged areal rainfall occurs during the rainy season from June through September compared to eighty percent for CFSR and only 40 % for TRMM.

Thus the TRMM 3B42 satellite rainfall data does not capture the temporal variation of rainfall well for the two basins. The poor seasonal rainfall predictions will cause the misrepresentation of watershed discharge, with nearly 82 and 83 % of annual discharge occurring between June through September for Gilgel Abay and Main Beles, respectively. Apparently, the TRMM 3B42 bias is adjusted with monthly gauged rainfall data, and as a result, has performed well in many parts of the world (Ouma et al., 2012; Javanmard et al., 2010). Dinku et al. (2008) and Haile et al. (2013), also in the Ethiopian highlands, have indicated a consistent result with our study. Haile et al. (2013) after personal communication with TMPA research team indicated that gauged rainfall data of the Upper Blue Nile Basin was not made available to them when the bias adjustment was conducted; therefore, further adjustment has to be done to use TRMM 3B42 rainfall products in the Blue Nile Basin. Likely, the additional adjustments will correct the seasonal distribution of rainfall in the Gilgel and Main Beles watersheds.

3.2 Simulated runoff using PED and HBV models

3.2.1 Simulation of stream discharge with PED model

The calibrated PED models using gauged rainfall or CFSR rainfall could represent the observed daily stream flow reasonable well for both the calibration and validation periods for the Gilgel Abay basin ($0.81 > \mathrm{NSE} > 0.60$) and the Main Beles ($0.81 > \mathrm{NSE} > 0.60$), see Fig. 5 and Table 2. For both basins, as demonstrated in Fig. 6

in which the average monthly values are depicted, the gauged rainfall gave slightly better results than the CFSR data (Fig. 7a and b). For the daily values the same trend is observed in which the regression coefficient indicated that during the validation period of the Gilgel Abay basin, the gauged rainfall could explain 82 % of the observed runoff variation and CFSR data could capture 73 % of the flow variation (Table 2). TRMM rainfall data could not characterize the observed discharge pattern (Figs. 5 and 7c) even with optimum model calibration mean observed flow is better representative than the simulated flow as indicated by NSE values close to zero (Table 2).

We found that the PED model parameters of the fractional areas, the half-life of the baseflow and the duration of the interflow after a rainstorm are sensitive for the prediction of stream discharge using either of the three rainfall records similar to Tilahun et al. (2013b). The model is insensitive to the maximum soil moisture storage for either of three regions (periodically saturated bottom lands, degraded soils, and permeable hillside). The reason is that, for a monsoon climate during the rainy phase, the soil does not dry out once wet, only during the first rains the discharge is affected by the amount of the water that can be stored in the soils. Therefore we kept, maximum water storages remained the same for all simulation.

Table 2 lists the optimised sensitive PED model parameter sets for the gauged, CFSR and TRMM rainfall estimate for Gilgel Abay and Main Beles basins. The calibrated model parameters for the subsurface flow represented by the half-life ($t_{1/2}$) and interflow calibration parameter τ^* for the different rainfall input data are almost the same for all simulations as expected and consistent with values used in simulation of Anjeni and Blue Nile Basins (Tilahun et al., 2013a). The fractional regions contributing to rapid subsurface and overland flow have different values for the gauged rainfall and CFSR rainfall data simulation. The total contributing area for the gauged rainfall adds up to 97 % for Gilgel Abay and 90 % for Main Beles. It is also consistent with earlier studies of PED simulation for a wide scale of watersheds study areas Tilahun et al. (2013b) indicated that the fractional area's for a 180 000 km^2 Blue Nile Basin adds up to 100 % while the smaller watershed of less than 5 km^2 are in the order of 60 %. So, for a midrange watershed area in a range of 1000 km^2 the fraction area up to 90 to 97 % would be realistic. Using the CFSR the fractional area adds up to 60 % for the Gilgel Abay and 42 % for the Main Beles. A fractional area of 1 would mean that all rainwater minus evaporation over the long-term becomes discharge at the outlet.

3.2.2 Simulation of stream discharge with HBV model

The semi-distributed HBV model has seven parameters controlling the total volume and shape of the hydrograph; there level of model parameter sensitivity is documented in Wale et al. (2009). The model is calibrated manually first by volume controlling parameters (FC, LP and Beta) followed by calibrating the shape controlling parameters (Alpha, PERC, K4 and K). The optimized model parameter sets of both watersheds and simulated discharge vs. observed runoff for gauged rainfall, TRMM and CFSR data of Gilgel Abay is shown in Table 3 and Fig. 8 respectively.

The simulated data for the calibration period using the gauged rainfall and CFSR indicated a fair to good performance with a daily NSE performance indicator equals to 0.81 and 0.72 for Gilgel Abay and 0.64 and 0.61 for Main Beles, respectively, and with a reasonable R^2 and PBIAS (Table 3, Fig. 10a and b). The simulation for both gauged rainfall and CFSR data captured well the base flow, the rising and recession limb of the hydrograph. Figure 9 depicts the long-term monthly average observed flow and simulated flow for gauged rainfall, TRMM and CFSR rainfall estimate of Gilgel Abay and Main Beles basins.

The peak flow is better captured by the CFSR data than the gauged rainfall although both simulation by gauged and CFSR rainfall underestimate very high single peaks that are commonly caused by extreme high rainfall events. For the study period, in the Gilgel Abay watershed there are 505 days with observed flow above 200 m^3 s^{-1}, the simulation by the CFSR rainfall estimate has captured 340 events and the gauged rainfall has captured 235 events. The optimized model parameters of the gauged rainfall and CFSR data have similar values except for FC and PERC in both watersheds (see

Table 3). Field capacity (FC) of the calibrated model using CFSR data is larger than the FC value of model calibrated by gauged rainfall (1480 and 245 mm for Gilgel Abay and 1400 and 800 mm for Main Beles). The FC value for the CFSR model simulation indicated that the soil retained greater quantities of water and released it afterwards by evapotranspiration and base flow compared to the gauged flow simulation, and it is the models way to deal with the greater amounts of rainfall in the CFSR data compared to the gauged. The increase FC will cause an increase in baseflow, and this has a counter effect on the percolation parameter (PERC). The optimised model parameter set is tested for independent data from 2004 to 2006 and the result is acceptable for both gauged rainfall and CFSR data for the study watersheds.

For this specific area and study period the TRMM 3B42 rainfall estimate did not perform well in capturing the observed flow of Gilgel Abay and Main Beles through model calibration as indicated statistically by the NSE values (Table 3) and visually in Fig. 10c and 7c.

3.2.3 Evaluation of rainfall products using HBV and PED models

The semi-distributed hydrological models HBV and PED are considered parsimonious models because they have a limited number of model parameters, making the calibration procedure less complicated and avoiding the problem of overparamterization. Most of the time calibration with a large number parameters leads to over parameterization (Whittaker et al., 2010) leading to a poor prediction accuracy. Parsimonious models are favourable compared to more complex models since they often perform as well as sophisticated ones (Duan et al., 1992).

Both models have reasonably captured the observed runoff for gauged rainfall and CFSR rainfall estimate as a model input for calibration and validation period for Gilgel Abay and Main Beles. The performance of both models on Main Beles watershed by gauged rainfall and CFSR data is close compared to the case of Gilgel Abay. This is because, ground rainfall gauging stations in the Main Beles are scares compared to Gilgel Abay (Fig. 1), and there is no rainfall observation station inside the watershed. So, it was difficult to capture the observed flow through model calibration using gauged rainfall in the Main Beles. This indicates that CFSR data can be an alternative to gauged rainfall as input to hydrological modelling when the rainfall station network is less dense. The peak flow for both models is better captured by the CFSR rainfall data than the gauged rainfall for obvious reason of 20 and 36 % additional rainfall for Gilgel Abay and Main Beles respectively. The simulation by the gauged rainfall underestimate very high single peaks that are commonly caused by extreme high rainfall events. The TRMM rainfall predictions has failed to perform within the objective function for both models.

4 Conclusions

This study has assessed the performance of commonly used high-resolution satellite rainfall products Climate Forecast System Reanalysis (CFSR) and Tropical Rainfall Measuring Mission (TRMM) 3B42 version 7 as input to a semi-distributed hydrological model HBV and PED for daily stream flow simulation in the Gilgel Abay and Main Beles basins, Ethiopia. The simulation is also done for the gauged rainfall to capture the observed flow through model parameter calibration. The gauged rainfall has performed well for both calibration and validation period with a fair to good NSE and on average the simulation has explained approximately 80 % of the observed flow variation through model calibration for both models. Rainfall estimate from the CFSR has also captured the observed flow though model calibration with a fair to good NSE and on average the CFSR runoff simulation has captured approximately 75 % of the variation of the observed flow for both models through model calibration. PED and HBV models through model calibration have responded for the extra rainfall of CFSR satellite rainfall estimate it has compared to the gauged rainfall. In HBV model, the maximum soil moisture storage parameter (FC) was too large indicating a deeper hydraulically active soil increasing the storage capacity of the soil. In PED model the fractional contributing area for CFSR rainfall estimate adds up to 60 % for Gilgel Abay and 42 % for Main Beles

respectively, while the fractional contribution area for the gauged rainfall is 97 and 90 % for Gilgel Abay and Main Beles. The TRMM data was not able to capture the observed flow through model calibration for both HBV and PED models. Therefore, we suggest further calibration of TRMM 3B42 rainfall product using the gauged rainfall for the Blue Nile area before the data is used for any application in the area.

Although only one station is available in the Gilgel Abay watershed and no rainfall station in the Main Beles basin, the performance of the gauged rainfall in capturing the observed runoff is better than both TRMM and CFSR estimates for calibration as well as validation periods. This indicates that gauged rainfall has its merit, but for remote regions with few or no observation stations in the Blue Nile area, CFSR rainfall estimate can be used to complement gauged rainfall data scarcity. The fractional saturated and degraded area of the PED model can be validated through satellite imagery by supervised land use classification. The simulation by the CFSR data for both HBV and PED models was able to capture the peak flows better than the runoff simulation by the gauged rainfall. So, the CFSR data might be more suitable to predict extreme events when using either PED or HBV models.

Acknowledgements. This research was supported by a graduate student fellowship for the senior author by the Norman E. Borlaug Leadership Enhancement in Agriculture Program funded by USAID and the International Water Management Institute. We are very grateful to the Ethiopian Ministry of Water, Irrigation and Energy and National Meteorological Agency of Ethiopia for providing daily river flow and metrological data for multiple stations free of charge. The data providers of Tropical Rainfall Measuring Mission (TRMM) product (3B42) and Climate Forecast System Reanalysis (CFSR) are also acknowledged.

References

Bayabil, H. K., Tilahun, S. A., Collick, A. S., Yitaferu, B., and Steenhuis, T. S.: Are runoff processes ecologically or topographically driven in the (sub) humid Ethiopian highlands? The case of the Maybar watershed, Ecohydrology, 3, 457–466, 2010.

Bitew, M. M., Gebremichael, M., Ghebremichael, L. T., and Bayissa, Y. A.: Evaluation of high-resolution satellite rainfall products through streamflow simulation in a hydrological modeling of a small mountainous watershed in Ethiopia, J. Hydrometeorol., 13, 338–350, 2012.

Collischonn, B., Collischonn, W., and Tucci, C. E. M.: Daily hydrological modeling in the Amazon basin using TRMM rainfall estimates, J. Hydrol., 360, 207–216, 2008.

Conway, D.: The climate and hydrology of the Upper Blue Nile River, Geogr. J., 166, 49–62, 2000.

Dinku, T., Chidzambwa, S., Ceccato, P., Connor, S., and Ropelewski, C.: Validation of high-resolution satellite rainfall products over complex terrain, Int. J. Remote Sens., 29, 4097–4110, 2008.

Douglas-Mankin, K., Srinivasan, R., and Arnold, J.: Soil and Water Assessment Tool (SWAT) model: current developments and applications, T. ASABE, 53, 1423–1431, 2010.

Duan, Q., Sorooshian, S., and Gupta, V.: Effective and efficient global optimization for conceptual rainfall–runoff models, Water Resour. Res., 28, 1015–1031, 1992.

Fuka, D. R., Walter, M. T., MacAlister, C., Degaetano, A. T., Steenhuis, T. S., and Easton, Z. M.: Using the Climate Forecast System Reanalysis as weather input data for watershed models, Hydrol. Process., 28, 5613–5623, doi:10.1002/hyp.10073, 2014

Gupta, H. V., Sorooshian, S., and Yapo, P. O.: Status of automatic calibration for hydrologic models: comparison with multilevel expert calibration, J. Hydrol. Eng., 4, 135–143, 1999.

Haile, A. T., Habib, E., Elsaadani, M., and Rientjes, T.: Inter-comparison of satellite rainfall products for representing rainfall diurnal cycle over the Nile basin, Int. J. Appl. Earth Obs., 21, 230–240, 2013.

Hong, Y., Adler, R. F., Negri, A., and Huffman, G. J.: Flood and landslide applications of near real-time satellite rainfall products, Nat. Hazards, 43, 285–294, 2007.

Jarvis, A., Reuter, H. I., Nelson, A., and Guevara, E.: Hole-Filled Seamless SRTM Data V4, International Centre for Tropical Agriculture (CIAT), available at: http://srtm.csi.cgiar.org, 2008.

Javanmard, S., Yatagai, A., Nodzu, M. I., BodaghJamali, J., and Kawamoto, H.: Comparing high-resolution gridded precipitation data with satellite rainfall estimates of TRMM_3B42 over Iran, Adv. Geosci., 25, 119–125, doi:10.5194/adgeo-25-119-2010, 2010.

Kebede, S., Travi, Y., Alemayehu, T., and Marc, V.: Water balance of Lake Tana and its sensitivity to fluctuations in rainfall, Blue Nile basin, Ethiopia, J. Hydrol., 316, 233–247, 2006.

Lindström, G., Johansson, B., Persson, M., Gardelin, M., and Bergström, S.: Development and test of the distributed HBV-96 hydrological model, J. Hydrol., 201, 272–288, 1997.

Moriasi, D., Arnold, J., Van Liew, M., Bingner, R., Harmel, R., and Veith, T.: Model evaluation guidelines for systematic quantification of accuracy in watershed simulations, T. ASABE, 50, 885–900, 2007.

Nash, J. and Sutcliffe, J.: River flow forecasting through conceptual models: Part I – a discussion of principles, J. Hydrol., 10, 282–290, 1970.

Ouma, Y. O., Owiti, T., Kipkorir, E., Kibiiy, J., and Tateishi, R.: Multitemporal comparative analysis of TRMM-3B42 satellite-estimated rainfall with surface gauge data at basin scales: daily, decadal and monthly evaluations, Int. J. Remote Sens., 33, 7662–7684, 2012.

Saha, S., Moorthi, S., Pan, H.-L., Wu, X., Wang, J., Nadiga, S., Tripp, P., Kistler, R., Woollen, J., and Behringer, D.: The NCEP climate forecast system reanalysis, B. Am. Meteorol. Soc., 91, 1015–1057, 2010.

Sharma, S., Isik, S., Srivastava, P., and Kalin, L.: Deriving spatially distributed precipitation data using the artificial neural network and multilinear regression models, J. Hydrol. Eng., 18, 194–205, 2012.

SMHI: Integrated Hydrological Modelling System (IHMS), Manual Version 5.10, Swedish Meteorological and Hydrological Institute, Norrkoping, Sweden, 2006.

Steenhuis, T. S., Collick, A. S., Easton, Z. M., Leggesse, E. S., Bayabil, H. K., White, E. D., Awulachew, S. B., Adgo, E., and Ahmed, A. A.: Predicting discharge and sediment for the Abay (Blue Nile) with a simple model, Hydrol. Process., 23, 3728–3737, 2009.

Steenhuis, T. S., Tilahun, S. A., Elkamil, M., Atanaw, F., Worqlul, A., Ayana, E. K., Abiy, A. Z., Mulukken, M., Tesemma, Z. K., and Mohamad, Y. A.: Simulating discharge and sediment concentrations in the increasingly degrading Blue Nile Basin, in: Proceedings conference on science and technology towards the Development of East Africa, Bahir Dar University Institute of Technology, 17 and 18 May 2013, 291–299, 2013.

Tarekegn, D. and Tadege, A.: Assessing the Impact of Climate Change on the Water Resources of the Lake Tana Sub-Basin Using the WATBAL Model, CEEPA, University of Pretoria, Pretoria, 2006.

Taye, M. T. and Willems, P.: Temporal variability of hydroclimatic extremes in the Blue Nile basin, Water Resour. Res., 48, W03513, doi:10.1029/2011WR011466, 2012.

Tesemma, Z. K., Mohamed, Y. A., and Steenhuis, T. S.: Trends in rainfall and runoff in the Blue Nile Basin: 1964–2003, Hydrol. Process., 24, 3747–3758, 2010.

Thornthwaite, C. and Mather, J.: The water balance, in: Publications in Climatology, Drexel Institute of Technology, Centerton, 104 pp., Vol. 8, No. 1, 1955.

Tilahun, S. A., Guzman, C. D., Zegeye, A. D., Engda, T. A., Collick, A. S., Rimmer, A., and Steenhuis, T. S.: An efficient semi-distributed hillslope erosion model for the subhumid Ethiopian Highlands, Hydrol. Earth Syst. Sci., 17, 1051–1063, doi:10.5194/hess-17-1051-2013, 2013a.

Tilahun, S., Mukundan, R., Demisse, B., Engda, T., Guzman, C., Tarakegn, B., Easton, Z., Collick, A., Zegeye, A., and Schneiderman, E.: Asaturation excess erosion model, Trans. Am. Soc. Agr. Biol. Eng., 56, 681–695, doi:10.13031/2013.42675, 2013b.

Wale, A., Rientjes, T., Gieske, A., and Getachew, H.: Ungauged catchment contributions to Lake Tana's water balance, Hydrol. Process., 23, 3682–3693, 2009.

Wang, W., Xie, P., Yoo, S.-H., Xue, Y., Kumar, A., and Wu, X.: An assessment of the surface climate in the NCEP climate forecast system reanalysis, Clim. Dynam., 37, 1601–1620, 2011.

Whittaker, G., Confesor, R., Di Luzio, M., and Arnold, J.: Detection of overparameterization and overfitting in an automatic calibration of SWAT, T. ASABE, 53, 1487–1499, 2010.

Worqlul, A. W., Maathuis, B., Adem, A. A., Demissie, S. S., Langan, S., and Steenhuis, T. S.: Comparison of rainfall estimations by TRMM 3B42, MPEG and CFSR with ground-observed data for the Lake Tana basin in Ethiopia, Hydrol. Earth Syst. Sci., 18, 4871–4881, doi:10.5194/hess-18-4871-2014, 2014.

Yilmaz, K. K., Hogue, T. S., Hsu, K.-l., Sorooshian, S., Gupta, H. V., and Wagener, T.: Intercomparison of rain gauge, radar, and satellite-based precipitation estimates with emphasis on hydrologic forecasting, J. Hydrometeorol., 6, 497–517, 2005.

Table 1. Coefficient of Determination (R^2) areal gauged and satellite rainfall estimates for Gilgel Abay and Main Beles basins.

	Main Beles					Gilgel Abay			
Basin		TRMM	CFSR	Gauged	Basin		TRMM	CFSR	Gauged
Main Beles	TRMM	1.00			Gilgel Abay	TRMM	1.00		
	CFSR	0.09	1.00			CFSR	0.24	1.00	
	Gauged	0.12	0.90	1.00		Gauged	0.35	0.92	1.00
Gilgel Abay	TRMM	0.90			Main Beles	TRMM	0.90		
	CFSR		0.98			CFSR		0.98	
	Gauged			0.98		Gauged			0.98

Table 2. Optimized model parameter set of PED model and model performance for gauged rainfall, TRMM and CFSR data.

Description		Gilgel Abay			Main Beles		
		Gauged rainfall	TRMM	CFSR	Gauged rainfall	TRMM	CFSR
Fraction of saturated area (%)		0.06	0.03	0.06	0.02	0.01	0.02
Fraction of degraded area (%)		0.05	0.03	0.04	0.05	0.02	0.02
Fraction of hillside area (%)		0.86	0.9	0.5	0.73	0.9	0.38
$t_{1/2}$ (days)		45	45	45	18	100	21
$\tau*$ (days)		40	20	40	46	100	76
Calibration Period (1994–2003)	PBIAS (%)	−3.9	−55	10.2	4.2	27.7	1.0
	NSE	0.81	0	0.75	0.7	0.06	0.66
	R^2	0.82	0.19	0.77	0.7	0.1	0.66
Validation period (2004–2006)	PBIAS (%)	10	2.2	10	7.9	12.2	2.3
	NSE	0.75	−0.28	0.64	0.81	−1.26	0.65
	R^2	0.8	0.01	0.71	0.82	0.0	0.62

Table 3. Optimized model parameter set of HBV model and its performance for gauged rainfall, TRMM and CFSR data.

Description		Gilgel Abay			Main Beles		
		Gauged rainfall	TRMM	CFSR	Gauged rainfall	TRMM	CFSR
Alpha		0.4	1	0.5	0.8	0.6	0.6
Beta		0.8	1.0	1.0	1.0	2.0	1.0
FC		245	100	1480	800	300	1400
LP		0.99	0.99	0.99	0.7	0.82	0.95
PERC		1.3	0.54	0.08	0.4	0.4	0.4
K4		0.04	0.02	0.05	0.002	0.002	0.03
Khq		0.13	0.05	0.11	0.09	0.2	0.07
Calibration Period (1994–2003)	PBIAS (%)	4.24	46	2.81	2.6	37	0.41
	NSE	0.81	−0.16	0.72	0.65	0.00	0.63
	R^2	0.82	0.25	0.73	0.63	0.06	0.61
Validation period (2004–2006)	PBIAS (%)	−6.2	6.8	−4.8	1.64	44.2	5.0
	NSE	0.79	0.06	0.62	0.64	−0.11	0.63
	R^2	0.83	0.07	0.68	0.67	0.00	0.66

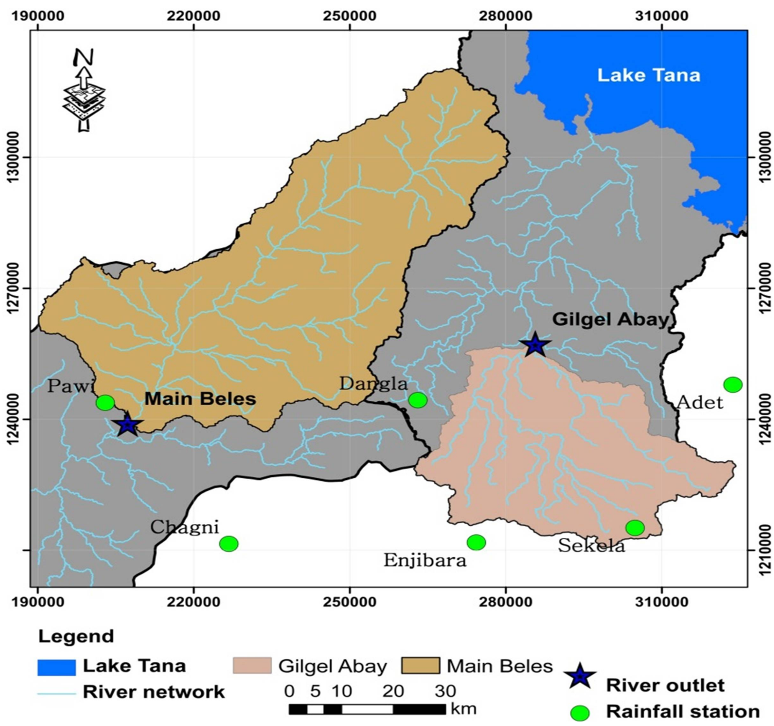

Figure 1. Drainage Pattern and meteorological station network of the Gilgel Abay and Main Beles basins.

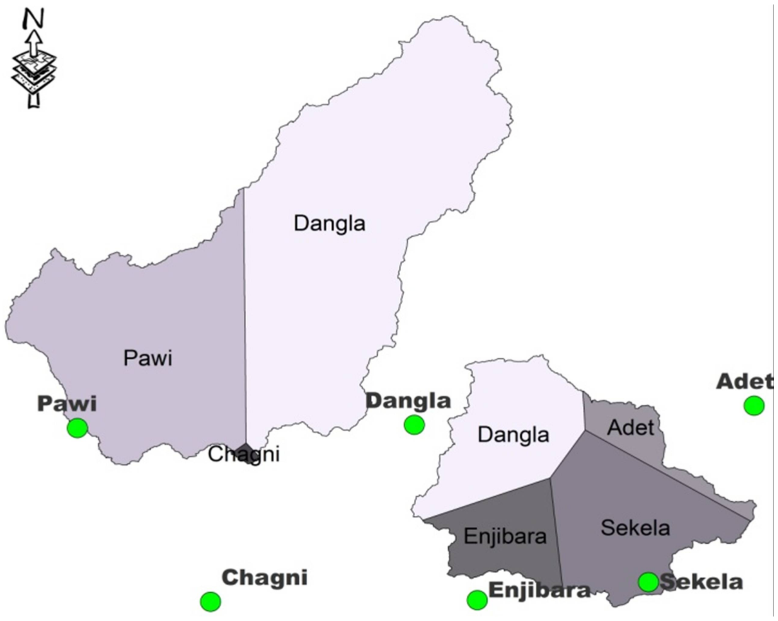

Figure 2. Thiessen Polygon map of the ground based rainfall stations in the Gilgel Abay and Main Beles basins.

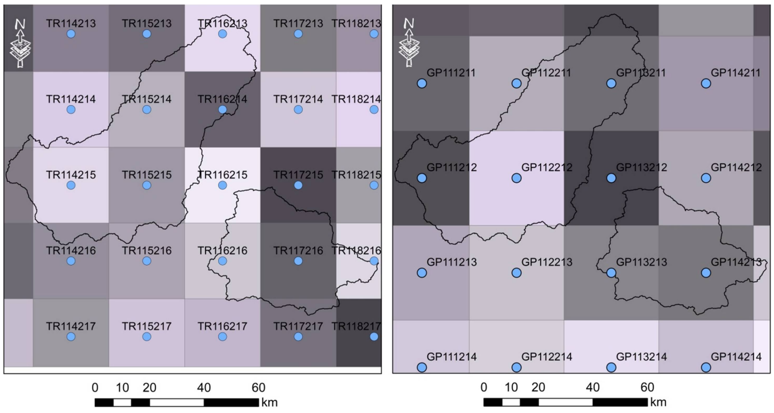

(A) TRMM

(B) CFSR

Figure 3. Satellite rainfall observation grid of **(a)** TRMM and **(b)** CFSR for Gilgel Abay and Main Beles basins. Grid size is approximately 27 and 38 km for TRMM and CFSR, respectively.

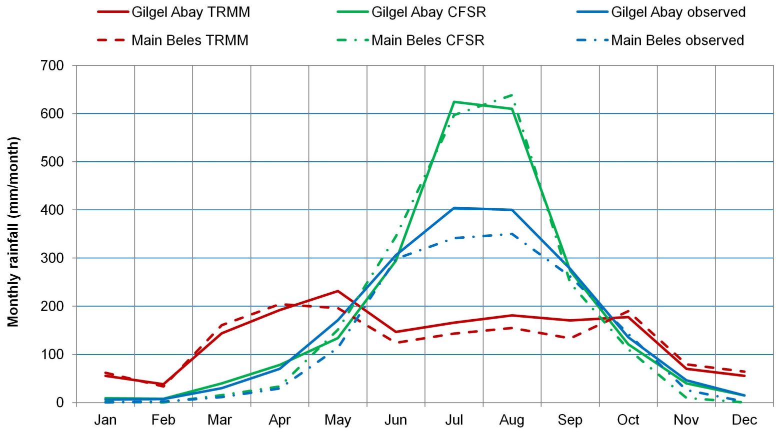

Figure 4. Long-term monthly average areal rainfall of gauged rainfall, CFSR data (1994–2003) and TRMM (1998–2003) for Gilgel Abay and Main Beles basins.

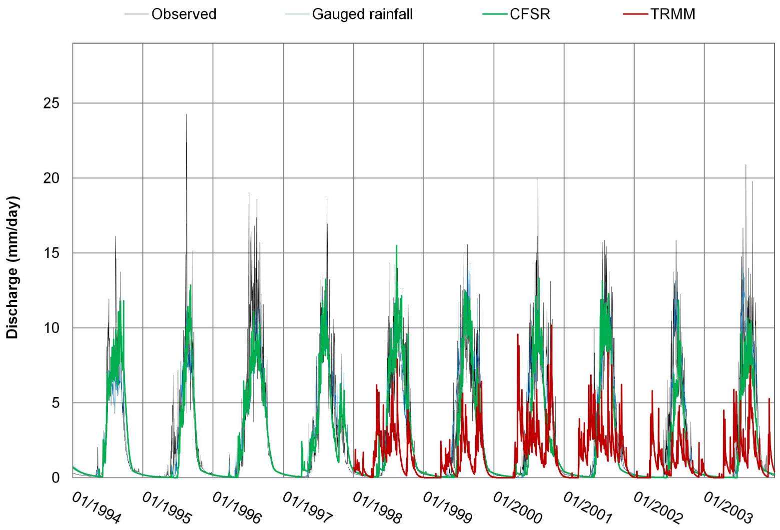

Figure 5. Simulated flow of PED model by gauged rainfall, TRMM and CFSR data plotted with observed flow for Gilgel Abay basin.

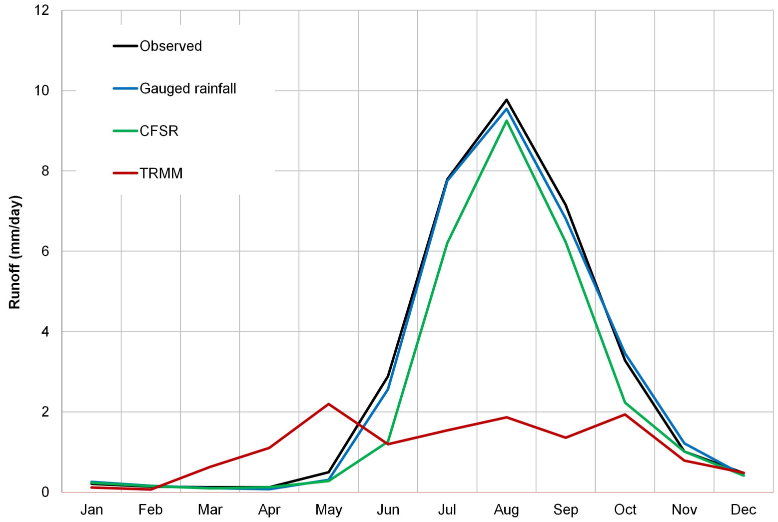

Figure 6. Comparison of long-term average monthly Gilgel Abay observed flow and PED simulation for gauged rainfall, CFSR (1994–2003) and TRMM rainfall estimate (1998–2003).

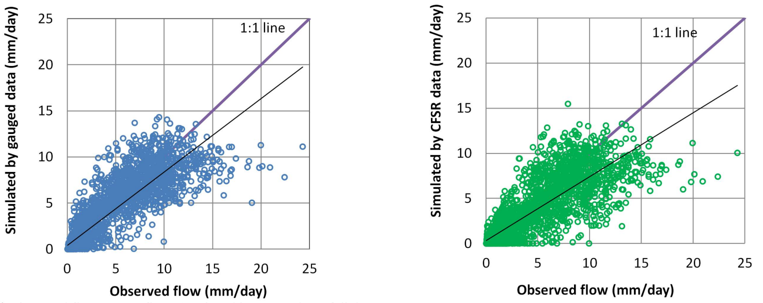

(a) Observed flow versus flow simulated by gauged rainfall data

(b) Observed flow versus flow simulated by CFSR data

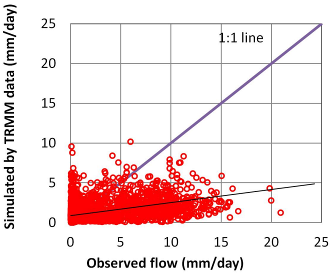

(c) Observed flow versus flow simulated by TRMM data

Figure 7. Correlation between observed flow and simulated flow for the calibration period using **(a)** gauged rainfall, **(b)** CFSR data and **(c)** TRMM data for the Gilgel Abay Basin using PED model.

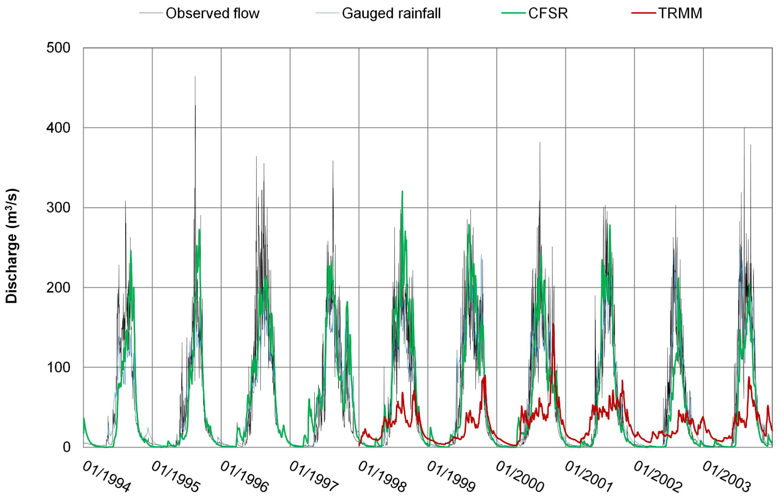

Figure 8. Simulated flow of HBV model by gauged rainfall, TRMM and CFSR data plotted with observed flow for Gilgel Abay basin (1994–2003).

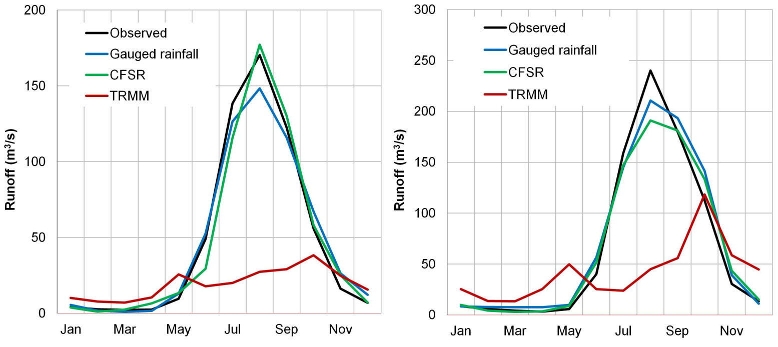

(A) Gilgel Abay (B) Main Beles

Figure 9. Comparison of long-term average monthly observed flow and HBV simulation for gauged rainfall, TRMM and CFSR rainfall estimate of **(a)** Gilgel Abay and **(b)** Main Beles basins.

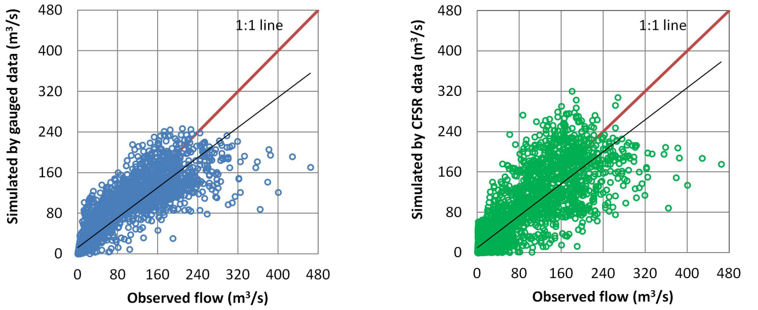

(a) Observed flow versus flow simulated by gauged rainfall data (b) Observed flow versus flow simulated by CFSR data

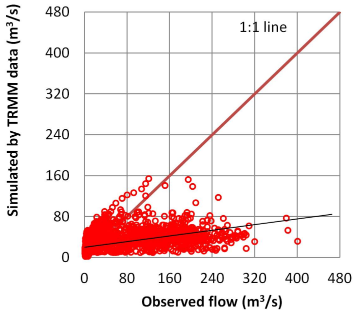

(c) Observed flow versus flow simulated by TRMM data

Figure 10. Correlation between observed flow and simulated flow for the calibration period using **(a)** gauged rainfall, **(b)** CFSR data and **(c)** TRMM data for the Gilgel Abay Basin using HBV model.